Insight into the Mechanism of Internalization of the Cell-Penetrating Carrier Peptide Pep-1 through Conformational Analysis†

Sébastien Deshayes,‡ Annie Heitz,§ May C. Morris,‡ Pierre Charnet,‡ Gilles Divita,‡ and Frédéric Heitz*,‡

CRBM-CNRS, FRE 2593, 1919 route de Mende, F-34293 Montpellier Cedex, France, and CBS-CNRS UMR 5048-INSERM UMR 554, Université de Montpellier 1, 15 Avenue Charles Flahault, F-34060 Montpellier, France

Received September 17, 2003; Revised Manuscript Received December 8, 2003

ABSTRACT: Recently, we described a new strategy for the delivery of proteins and peptides into mammalian cells, based on an amphipathic peptide of 21 residues, Pep-1, which was designed on the basis of a protein-interacting domain associated with a nuclear localization sequence and separated by a linker. This peptide carrier constitutes a powerful tool for the delivery of active proteins or peptides both in cultured cells and in vivo, without requiring any covalent coupling. We have examined the conformational states of Pep-1 in its free form and complexed with a cargo peptide and have investigated their ability to interact with phospholipids and the structural consequences of these interactions. From the conformational point of view, Pep-1 behaves significantly differently from other similarly designed cell-penetrating peptides. CD analysis revealed a transition from a nonstructured to a helical conformation upon increase of the concentration. Determination of the structure by NMR showed that in water, its α-helical domain extends from residues 4−13. CD and FTIR indicate that Pep-1 adopts a helical conformation in the presence of phospholipids. Adsorption measurements performed at the air−water interface are consistent with the helical form. Pep-1 does not undergo conformational changes upon formation of a particle with a cargo peptide. In contrast, we observe a partial conformational transition when the complex encounters phospholipids. We propose that the membrane crossing process involves formation of a transient transmembrane pore-like structure. Conformational change of Pep-1 is not associated with complexation with its cargo but is induced upon association with the cell membrane.

To circumvent the technological problems of gene delivery, an increasing interest is being taken in designing novel strategies to deliver full-length proteins into a large number of cells (*1*, *2*). However, the development of peptide-drugs and therapeutic proteins remains limited by the poor permeability and the selectivity of the cell membrane. Recently, substantial progress has been made in the development of cell-penetrating peptide-based drug delivery systems which are able to overcome both extracellular and intracellular limitations *(3*−*5*). A series of small protein domains, termed protein transduction domains (PTDs),[1] have been shown to cross biological membranes efficiently, independently of transporters and specific receptors, and to promote the delivery of peptides and proteins into cells *(6* and for a review see ref *7)*. Numerous studies strongly suggest that PTD-mediated transfection may have a major impact on the future of therapies against a variety of viral diseases and cancers. In particular, the Tat-derived peptide of immunodeficiency virus (HIV-1) (*6*, *8*), the third α-helix of Antennapedia homeodomain (pAntp) (*9*, *10*), VP22 protein of herpes simplex virus (*11*), transportan (*12*), and polyarginine sequences (*13*) have been successfully used to improve the delivery of covalently linked peptides or proteins into cells.

Recently, we have described a new strategy to deliver full-length proteins and peptides into mammalian cells, on the basis of use of a short amphipathic peptide carrier, Pep-1. We have demonstrated that this peptide carrier efficiently promotes the delivery and correct intracellular localization of a wide variety of peptides, proteins, and antibodies in their native, biologically active form into a broad spectrum of cell lines, without the need for prior chemical covalent coupling or denaturation steps (*14*). Pep-1 is a 21-residue peptide, consisting of three domains with specific functions: (i) a hydrophobic tryptophan-rich motif, forming the main interactions with macromolecules and required for efficient targeting to the cell membrane, (ii) a hydrophilic lysine-rich domain derived from the nuclear localization sequence (NLS) of simian virus 40 (SV-40) large T antigen, required to improve intracellular delivery and solubility of the peptide vector, (iii) and a spacer domain, which improves the flexibility and the integrity of both the hydrophobic and the hydrophilic domains (*14*). As Pep-1 does not deliver macromolecules through the endosomal pathway, their degradation is limited and their rapid dissociation from Pep-1 is enabled as soon as the cell membrane has been crossed. In addition, this peptide-based protein delivery strategy

† This work was supported by EU Grant QLK2-CT-2001-01451.

* To whom correspondence should be addressed. Phone: ++ 33 (0)4 67 61 33 92. Fax: ++ (0)4 67 52 15 59. E-mail: heitz@crbm.cnrs-mop.fr.

‡ CRBM-CNRS.

§ CBS-CNRS.

[1] Abbreviations: PTD, protein transduction domain; NLS, nuclear localization sequence; CPP, cell-penetrating peptides; pAntp: antennapedia homeodomain; DOPC, dioleoylphosphatidyl-choline; DOPG: dioleoylphosphatidylglycerol; DPPC, dipalmitoylphosphatidylcholine; DPPG: dipalmitoylphosphatidylglycerol; CMC, critical micellar concentration.

10.1021/bi035682s CCC: $27.50
Published on Web 01/22/2004

presents several advantages, including the rapid delivery of proteins into cells with very high efficiency, stability in physiological buffer, lack of toxicity, and lack of sensitivity to serum. As such, Pep-1 technology constitutes a powerful tool for basic research, and several studies have demonstrated its usefulness for studying the role of proteins, or for targeting specific protein/protein interactions in vitro as well as in vivo (*14*−*19*).

Recently the uptake mechanism of PTDs and cell-penetrating peptides (CPPs) has become very controversial, mainly due to the fact that very little is known concerning the active conformation of CCPs associated with membrane penetration and translocation. CPPs seem capable of adopting different secondary structures, depending on their environment. pAntp has been shown to adopt either helical or β strand structures and to induce formation of inverted micelles (*20*−*22*). Transportan adopts a helical structure in any environment (*21*). In contrast, Tat-derived peptide has not been shown to adopt any particular secondary structure, although it has been suggested that a helical structure is required for its uptake (*23*, *24*). Therefore, an important criterion to be considered in the process of investigating the mechanism of CCPs is the structural requirement for its cellular uptake. In the present work, we have combined a variety of physical and spectroscopic approaches to gain insight into the structure(s) involved in the formation of the Pep-1/cargo complexes and in the interactions of Pep-1 with lipids, and thus to characterize its mechanism of cellular internalization. We demonstrate that Pep-1 interacts strongly with membranes and adopts a helical conformation which is essential for the uptake mechanism. In contrast, formation of stable complexes between Pep-1 and a cargo peptide is not associated with any conformational changes. Taken together, these data enable us to gain insight into the mechanism of internalization of the cell-penetrating carrier peptide Pep-1, by providing a better understanding of the structural parameters which govern cellular penetration.

EXPERIMENTAL PROCEDURES

Materials. Peptides. Pep-1 (KETWWETWWTEWSQPKKKRKV), Pep-A (RGTKALTEVIPLTEEAELELAENREILKEPVH), and Pep-B (MEFSLKDQEAKVSRSGLYRSPSMPENLNRPRLKQVEKFKDNTIPDKKKC) were synthesized by solid-phase peptide synthesis using AEDI-Expansin resin on a 9050 PepSynthesizer (Millipore, Wartford, U.K.) according to the Fmoc/tBoc method, as already described (*14*, *25*). Peptides were acetylated at their N-terminus, and both bear a cysteamide group at their C-terminus.

Phospholipids. Dioleoylphosphatidylcholine (DOPC), dioleoylphosphatidylglycerol (DOPG), dipalmitoylphosphatidylcholine (DPPC), and dipalmitoylphosphatidylglycerol (DPPG) were purchased from Avanti Polar Lipids (Alabaster, AL).

Fourier Transform Infra-Red (FTIR) Spectroscopy. FTIR spectra were obtained on a Bruker IFS 28 spectrometer equipped with a liquid nitrogen cooled MCT detector. Spectra (1000−2000 scans) were recorded at a spectral resolution of 4 cm^{-1} and were analyzed using the OPUS/IR2 program. Samples were obtained by deposition of solutions of lipid and peptide mixtures onto a fluorine plate where the solvents were allowed to evaporate under a nitrogen flux.

Circular Dichroism (CD) Measurements. CD spectra were recorded on a Jasco 810 dichrograph in a quartz cell with an optical path of 1 mm for peptide in aqueous solutions. For samples transferred by the Langmuir−Blodgett (LB) method, quartz plates were used, and eight plates were gathered to amplify the detected signal. The band positions were determined after smoothing the spectra by applying the method of Savitzky-Golay.

NMR Spectroscopy. Samples were prepared by dissolving peptide in either 90% H_2O/10% ^2H_2O (v/v) or 100% ^2H_2O to a concentration of approximately 3 mM. For micelle-bound peptide, 2 mM peptide solution was mixed with 200 mM perdeuterated SDS. The pH of the samples was adjusted to 3.1 by addition of dilute HCl or NaOH.

All ^{1}H NMR spectra were recorded on a Bruker Avance-600 spectrometer. Data were acquired at 285, 295, and 305 K, and TSP-d4 was used as an internal reference. TOCSY and NOESY 2D experiments were performed according to standard procedures (*26*) using quadrature detection in both dimensions with spectral widths of 11.67 ppm in both dimensions. The carrier frequency was centered on the water signal, and for experiments recorded in H_2O, water resonance was suppressed by the WATERGATE method (*27*). 2D spectra were obtained using 1024 or 2048 points for each t1 value, and 512 t1 experiments were acquired. TOCSY spectra were recorded with spin lock times of 60 ms. Mixing time was 250 ms in NOESY spectra. Spectra were processed using XWINNMR (Bruker). The t1 dimension was zero filled to 1024 points, and shifted sine bell functions were applied in t1 and t2 domains for apodization prior to Fourier transform. A baseline correction was applied using a five order polynomial function. The assignment of all the ^{1}H resonances present in the spectrum was achieved using well-established techniques (*26*).

Adsorption at the Air−Water Interface. Adsorption studies at the air−water interface were carried out using a microtrough S and analyzed with the Film Ware 2.41 program from Kibron, Inc. (Helsinki, Finland). Measurements were made at equilibrium after injection of aliquots of an aqueous solution of peptide into the aqueous subphase, gently stirred with a magnetic stirrer. To determine the critical micellar concentration (CMC), this procedure was repeated until no further increase of the surface pressure could be detected.

For penetration measurements of the peptide into phospholipids, a lipid monolayer was initially obtained by spreading a solution of lipid in chloroform/methanol (3/1, v/v) onto the air/PBS aqueous solution interface in order to obtain a definite surface pressure. The solvent was allowed to evaporate, and when a constant surface pressure was reached, a small volume of the aqueous peptide solution was injected into the subphase beneath the lipid monolayer. Increases of surface pressure were recorded for different initial lipid surface pressures in order to determine the critical pressure of insertion (CPI) of the peptide into the lipid.

Langmuir−Blodgett Monolayers. All transfers onto quartz slides were achieved using a homemade setup with a procedure described previously (*28*, *29*). During LB transfers, the surface pressure was maintained constant through a feedback system, and the selected surface pressure was 5mN/m, a value close to that of the collapse pressure of pure Pep-1.

Fluorescence Titrations. Fluorescence experiments were performed on a PTI spectrofluorimeter. All fluorescence measurements were performed at 25 °C. Intrinsic tryptophan fluorescence of Pep-1 was routinely excited at 295 nm in order to minimize the substrate inner-filter effect, and the emission spectrum was recorded between 310 and 380 nm, with a spectral band-pass of 2 and 8 nm for excitation and emission, respectively. A fixed concentration of peptide vector (1 μM) was titrated by increasing the concentration of cargo peptide (from 0 to 1 μM) or of vesicles of phospholipids. The latter experiments were carried out in water, while the former were performed in phosphate buffer pH 6.5 containing 20 mM KH_2PO_4, 25 mM K_2HPO_4, 1 mM EDTA, 100 or 300 mM NaCl. All measurements were corrected for the equipment and the dilution and curve fitting was performed as already described (*30*).

Electrophysiological Recordings on Xenopus laevis Oocytes. Ovaries were surgically removed from *Xenopus laevis* females (Elevage de Lavalette, Montpellier, France), and oocytes were isolated after enzymatic dissociation (collagenase, type IA, Sigma, La Verpillere, France) and extensive washing, as already described (*31*). After 24 h, oocytes were placed individually in a 50 μL recording chamber. Macroscopic whole-cell currents were recorded under two electrode voltage-clamp using the GeneClamp 500 amplifier (Axon Instr., Union City, CA) connected to the bath with the virtual-ground bath-clamp headstage and 3M KCl agar-bridges. Voltage and current electrodes were filled with 3 M KCl and had a resistance of 1−2 MΩ. Junction potentials (typically less than 3−5 mV) were canceled. Voltage-command, sampling, acquisition, and analysis were done using a Digidata 1200 and the pClamp program (version 6.01, Axon Instruments). All experiments were performed at room temperature (20−25 °C).

The recording solution had the following composition (in mM): NaCl, 100; Hepes, 10; $MgCl_2$, 2; pH 7.2 with NaOH. Pep-1 was applied directly to the bath at the final concentration (10 μM). Membrane current was recorded during voltage-ramps (−80 to +80 mV, 450 ms), applied from the holding potential of −80 mV every 5 s. Reversal potentials were measured as the zero-current potential after digital subtraction of traces recorded before and after Pep-1 application.

RESULTS

With the aim of gaining insight into the mechanism of internalization of the cell-penetrating carrier Pep-1, we investigated whether penetration was dependent on a particular conformational state of this peptide and whether this conformation was promoted through association with its cargo or upon interaction with phospholipids.

Structural Characterization of the Free and Detergent-Bound Forms of Pep-1. We first examined the structural characteristics of Pep-1 peptide in its free form by circular dichroism and found that its conformation varied with its concentration. For a concentration ranging between 0.1 and 0.3 mg/mL, the CD spectrum showed a single negative band centered at 202 nm associated with a shoulder around 220 nm (Figure 1; spectrum 1), suggestive of a nonstructured or poorly ordered structure. Interestingly, increasing the concentration of Pep-1 up to 3 mg/mL promoted dramatic

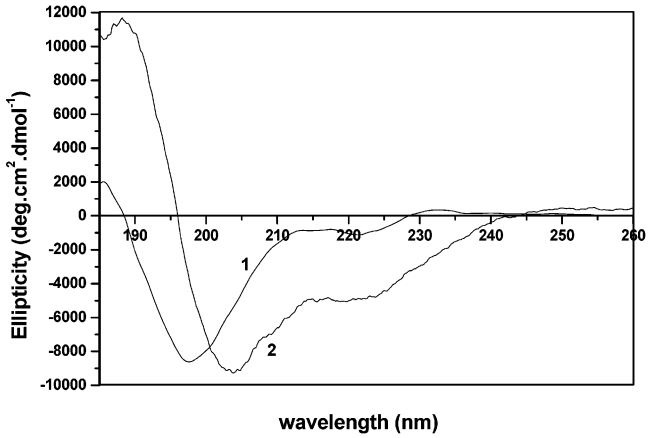

FIGURE 1: Concentration dependence of the far UV CD spectrum of Pep-1. Spectrum 1, $c = 0.3$ mg/mL; spectrum 2, $c = 3$ mg/mL.

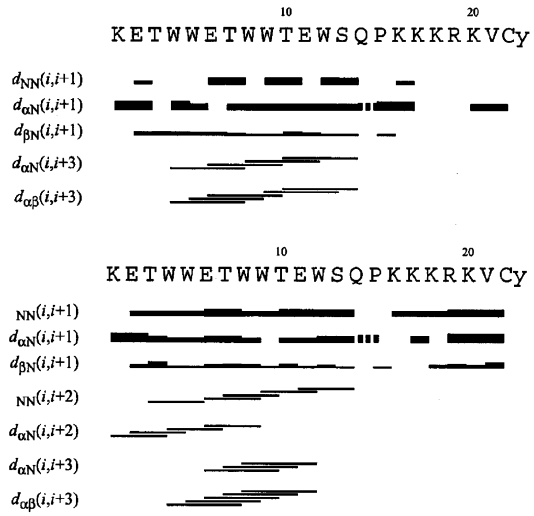

FIGURE 2: Summary of NMR data−sequential and medium range NOE connectivities (top, Pep-1 in H_2O; bottom, Pep-1 in SDS d_{25}). Dashed lines indicate the sequential Hα−Hδ(i,i+1) connectivities for the proline residue. The height of the bar corresponds to the strength of the NOE.

modifications which yielded a spectrum characterized by a minimum at 205 nm, a pronounced shoulder at 221 nm, and a maximum at 190 nm (Figure 1; spectrum 2), representative of a helical conformation (*32*). This tendency for Pep-1 to adopt, at least in part, a helical structure was confirmed by observations in SDS-containing media. Indeed, above the CMC of the detergent, a spectrum with two minima at 207 and 222 nm and a maximum at 192 nm was obtained (data not shown), typically characteristic of a helical conformation.

To further understand how Pep-1 was folded in solution and determine which residues were involved in helical conformations, we characterized the secondary structure of Pep-1 in solution by NMR. The sequential and medium range NOEs observed for Pep-1 in H_2O and Pep-1 in the presence of SDS are summarized in Figure 2. The detection of strong dNN, dαN(i,i +3) and dαβ(i,i+3) NOEs for Pep-1 in H_2O in the segment 4−13 is consistent with the existence of a helical secondary structure in this part of the sequence (Figure 2, top). In the presence of SDS, dNN, dNN(i,i+2), dαN(i,i+3), and dαβ (i,i+3), NOEs characteristic of a helix were observed for the same segment (residues *4*−*13*). In addition, several dαN(i,i+2) NOEs detected at the beginning of the sequence are indicative of a 3_{10} helix (Figure 2 bottom).

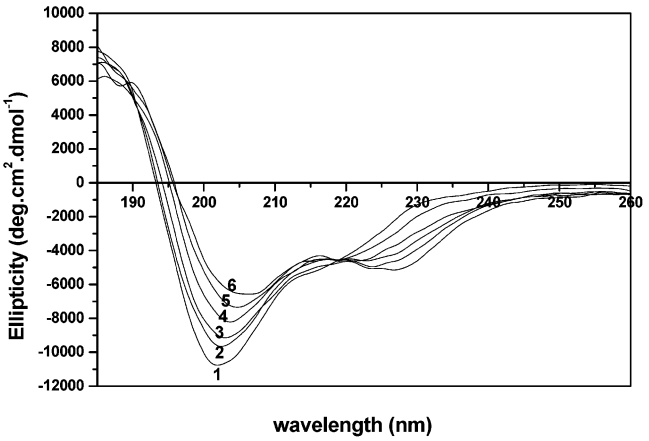

FIGURE 3: Influence of the presence of vesicles of DOPC-DOPG (80−20) on the far UV CD spectrum of Pep-1. The peptide/lipid ratios are 1/0, 1/1, 1/3,1/4, 1/6, and 1/7 for the spectra 1−6, respectively.

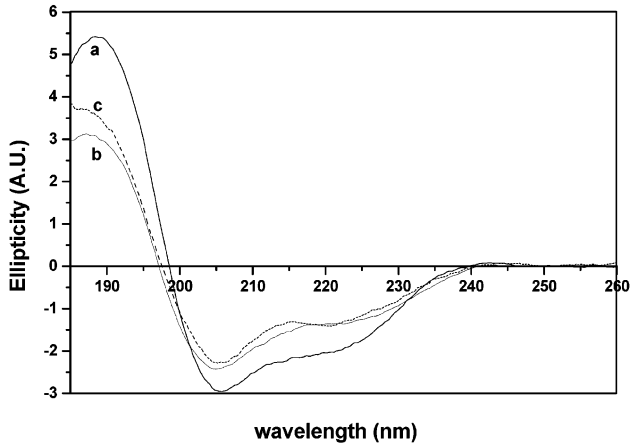

FIGURE 4: Far UV CD spectra of transferred Pep-1 containing monolayers. Spectrum a, pure peptide; spectra b and c, in the presence of DOPG or DOPC at a peptide/ lipid ratio of 0.25, respectively.

The extension of the helical structure to the N-terminus of Pep-1 in medium containing SDS is the only difference observed between the conformation of Pep-1 in H_2O and Pep-1 in SDS micelles. Interestingly, the NLS moiety of Pep-1 remained unstructured in both media.

Structural Characterization of Pep-1 in the Presence of Phospholipids. To determine whether the interaction of Pep-1 with an environment mimicking the cell membrane had any effect on its conformational state, we characterized the structural states of Pep-1 by CD in the presence of phospholipids. As shown in Figure 3, we found that successive addition of vesicles of DOPC/DOPG 80/20 to a dilute solution of Pep-1 in water induced a structural transition. Owing to the existence of isodichroic points around 220 nm, the various behaviors correspond to transitions between two states. The first state corresponds to a nonstructured form, while the second is more difficult to identify unambiguously due to the presence of 5 Trp residues which are most likely involved in the contribution at 228 nm. Nevertheless, since the spectra always show a maximum at about 191 nm and a minimum located in the 206−208 nm range, with no minimum between 215 and 220 nm, the presence of a β sheet structure can be ruled out, and these data therefore also suggest that the conformation of Pep-1 is helical in the presence of phospholipids. The helical structure adopted by Pep-1 in the presence of phospholipids was confirmed by CD observations performed on peptide-containing transferred monolayers (Figure 4) (*33*). In all cases, with or without any type of lipid, whether neutral or negatively charged, the spectra exhibit two minima at 206 and 222 nm and one maximum around 190 nm, thereby identifying a helical structure as the major structural component.

To obtain more details on the structure of Pep-1 in the presence of phospholipids, an FTIR study was undertaken. As shown in Figure 5, all spectra showed a complex contour of the Amide I band. In the absence of lipids and at low lipid/peptide ratio (DOPC), two distinct contributions were observed, one at 1625−1630 cm^{-1} and the other centered at 1655−1660 cm^{-1}. An increase of the DOPC/peptide ratio generated a significant decrease of the 1625 cm-1 contribution associated with a broadening of the 1655−1660 cm^{-1} contribution (*34*). Similar results were obtained with DOPG instead of DOPC (data not shown). The low-wavenumber

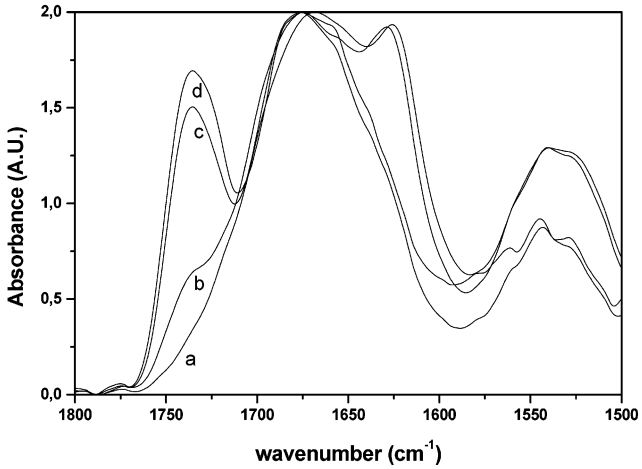

FIGURE 5: FTIR spectra (Amide I and II region) of Pep-1/ phospholipid mixtures at various peptide/lipid ratios. Spectra a−d correspond to peptide/lipid ratios of 1/0, 1/1, 1/10, and 1/20, respectively.

Amide I band contribution which was only observed in the absence of lipids and for a low lipid/peptide ratio can be unambiguously assigned to a β-sheet structure. However, the other contribution reflects the presence of a conformational mixture. The finding of a broad band is in full agreement with the NMR data obtained in SDS (see above) and indicates that two helical forms are maintained in a lipidic medium. (1655 cm^{-1}, α-helix; 1665 cm^{-1}, helix 3_{10}) (*35*, *36*).

Studies at the Air−Water Interface and Penetration Experiments. With our knowledge of the structural characteristics of Pep-1 in its free form and in the absence or in the presence of phospholipids, we next investigated its physical properties with respect to interactions with and penetration into lipid monolayers.

Before measuring the ability of Pep-1 to penetrate into lipidic media by the monolayer approach, we determined the saturating surface pressure induced by the peptide at a lipid-free air−water (0.154 M NaCl) interface. The variation of the surface tension as a function of the peptide in the subphase is shown in the inset of Figure 6. This variation shows that saturation is obtained at a concentration of 5 10^{-7} M Pep-1 and that the corresponding surface tension is rather

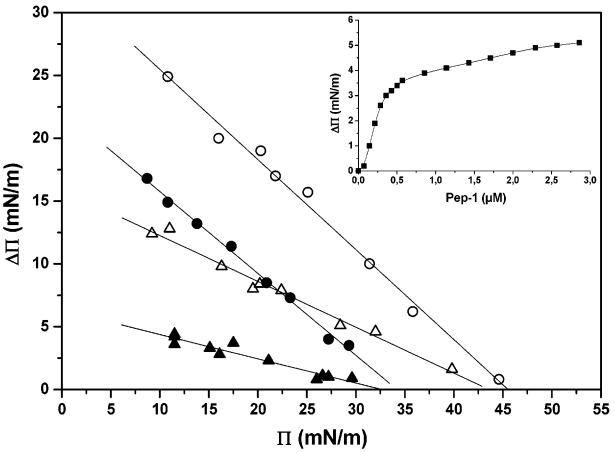

FIGURE 6: Variation of the surface pressure as a function of the initial surface pressure of the phospholipid monolayer. (△) DOPC, (○) DOPG, (●) DPPG, and (▲) DPPC. Extrapolation at zero initial pressure gives the critical pressure of insertion. Inset: variation of the peptide-induced surface pressure as a function of the peptide concentration in the subphase in the absence of phospholipid.

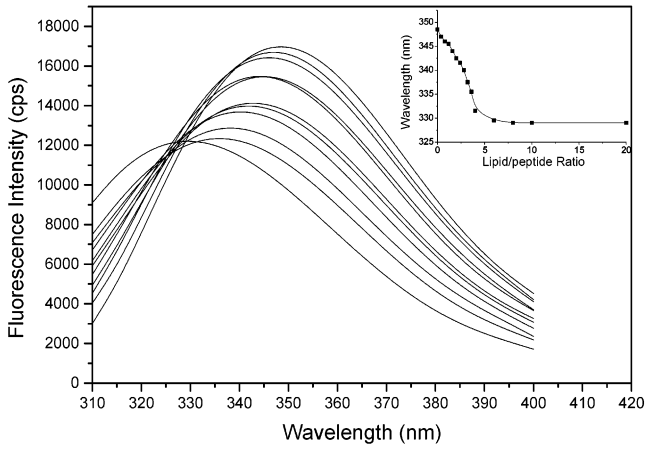

FIGURE 7: Effect of the addition of phospholipid vesicles on the fluorescence of the Trp residues of Pep-1. The various spectra correspond to the peptide/lipid ratio quoted on the inset which shows the variation as a function of the peptide/lipid ratio of the wavelength corresponding to the maximum of the fluorescence emission.

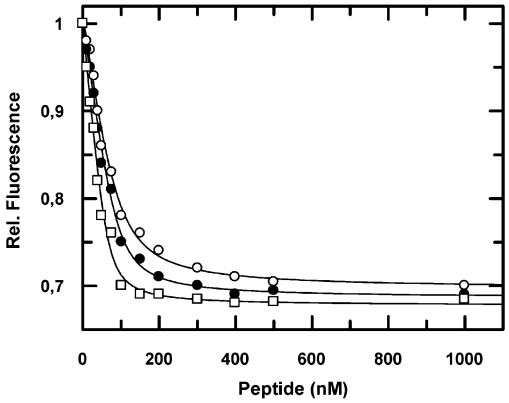

FIGURE 8: Formation of Pep-1/peptide complex. The formation of Pep-1/peptide complexes was monitored by following changes in intrinsic tryptophan fluorescence of Pep-1 at 340 nm, upon excitation at 295 nm. A fixed concentration of Pep-1 (1 μM) was titrated with increasing concentrations of peptide A in the presence (○) or in the absence (□) of 200 mM NaCl or with increasing concentrations of Pep-B (●).

low (4 mN/m) compared to other cell-penetrating peptides studied previously in our laboratory (>15 mN/m) (*37*, *38*). Such a low increase of the surface tension indicates that Pep-1 has a weak amphipathic character.

To investigate the ability and understand the mechanism through which Pep-1 penetrates into membranes, we performed penetration experiments using phospholipds in the liquid expanded (DOPC and DOPG) or liquid condensed (DPPC and DPPG) states. In the case of liquid-expanded monolayers, a strong increase in the surface pressure was observed. The most important characteristics of these experiments lie in the fact that (i) both DOPC and DOPG yielded identical cpi (45 mN/m) and that (ii) extrapolations at zero initial pressure were high (16 and 32 mN/m for DOPC and DOPG, respectively), and significantly different from that measured in the absence of lipid (Figure 6). For the two other phospholipids, DPPC and DPPG, again the cpi is high (33 mN/m) and does not depend on the nature of the headgroups. However, from examination of the extrapolation at an initial pressure of zero, it appears that the difference lies mainly in the poor interaction of the peptide with DPPC as compared to DPPG. The high values found for the cpi suggest that the Pep-1 can spontaneously insert into natural membranes (*39*). Extrapolations at zero initial pressure provide a good indication that strong peptide-lipid interactions can occur at least in monolayers, with all lipids except DPPC.

Penetration into Phospholipid Vesicles. Penetration of Pep-1 into phospholipid bilayers was investigated by fluorescence spectroscopy. Pep-1 contains five Trp residues in its hydrophobic moiety, which represent sensitive probes for monitoring interactions and changes in its environment upon penetration into phospholipid bilayers by intrinsic fluorescence. As reported in Figure 7, successive additions of phospholipid vesicles to a solution of Pep-1 induced significant changes in the fluorescence spectrum. Indeed, a continuous shift of the fluorescence maximum (from 350 to 328 nm) accompanied by quenching of fluorescence occurred when the lipid/peptide ratio was increased from 0 to 5, and no further change occurred above this ratio. The blue shift of fluorescence is consistent with a change in the environment of the Trp residues from polar to nonpolar in the presence of phospholipid vesicles (*40*). This is a good indication that the Trp residues are embedded in the lipidic core when Pep-1 encounters a membrane. In addition, quenching is suggestive of a transfer between Trp residues which are engaged in clusters when the peptide adopts a helical structure.

Formation of Peptide Vector/Peptide Cargo Complexes—Structural Consequences. We finally studied the ability of Pep-1 to interact with Pep-A, a 32-mer cargo peptide by intrinsic tryptophan fluorescence spectroscopy, and investigated the structural consequences of this interaction by CD. We first verified that in the absence of other proteins or peptides, the fluorescence of Pep-1 varied linearly with its concentration up to a concentration of 1 10^{-4} M, indicating that it does not self-associate in the conditions used for in vitro titration and cell delivery experiments (data not shown). As shown in Figure 8, binding of Pep-A peptide to Pep-1 induced a marked quenching of the intrinsic tryptophan fluorescence of Pep-1, with a saturating value of 36%. Moreover, this interaction resulted in a blue shift of the fluorescence emission maximum of 11 nm, (from 350 to 339

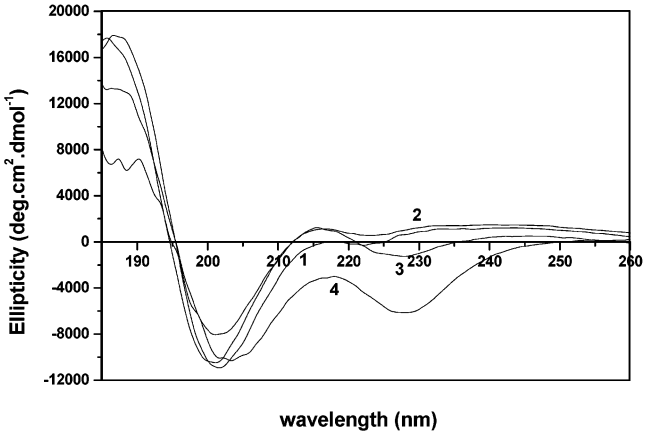

FIGURE 9: Phospholipid-induced modification of the far UV CD spectrum of the Pep-1/peptide A (5/1) complex. Spectra 1−4 correspond to lipid/peptide ratios of 0, 2, 10, and 100, respectively.

nm, data not shown), suggesting that the Trp residues of Pep-1 interact directly with the cargo peptide Pep-A. Saturation was reached at a concentration of 200 nM, that is, 5-fold lower than that of the Pep-1 (1 μM), suggesting that the cargo peptide interacts with more than one molecule of Pep-1 peptide vector. We also found that the interaction between Pep-1 and Pep-A remained stable at high salt concentrations (300 mM NaCl), revealing that binding to Pep-1 mainly involves hydrophobic contacts (Figure 8). Taking into account the number of Pep-1 molecules bound to the cargo peptide Pep-A, the dissociation constant was estimated to be in the range of 120 ±50 nM, indicating that when Pep-1 is mixed with a peptide in solution they associate rapidly into noncovalent stable complexes through hydrophobic interactions. To check that this behavior is not specific to Pep-A, this experiment was repeated using Pep-B whose sequence strongly differs from that of Pep-A (Figure 8) and led to the same conclusion.

We next examined whether the interaction of Pep-1 with a cargo peptide had any effect on the structural characteristics of Pep-1. As shown in Figure 9, addition of Pep-A which is nonstructured whatever the medium to a solution of Pep-1 did not yield any modifications in the CD spectrum of Pep-1.

Finally, to complete our understanding of the relationship among the interactive ability of Pep-1 with its cargo, its penetrating capacity, and its conformational state, we examined whether the presence of phospholipids induced any structural modifications on Pep-1 complexed to its cargo, similar to those already detected for Pep-1 in its free form. Upon addition of vesicles made of DOPC/DOPG (80/20) to a preformed Pep-1/Pep-A complex, the modifications of the CD spectrum show the same trend as those obtained for free Pep-1 to which lipid vesicles were added (see Figure 3). This result indicates that the particle formed by complexes of Pep-1 and its cargo interacts with lipid bilayers and that this interaction promotes, at least in part, a conformational transition of Pep-1 to an α-helical form.

Toward a Model Accounting for Translocation Properties: Electrophysiological Measurements. When Pep-1 (10 μM) was applied to voltage-clamped oocytes, a marked increase in membrane conductance was recorded. This increase was best visualized by an increase in membrane current recorded during voltage ramps applied from −80 mV

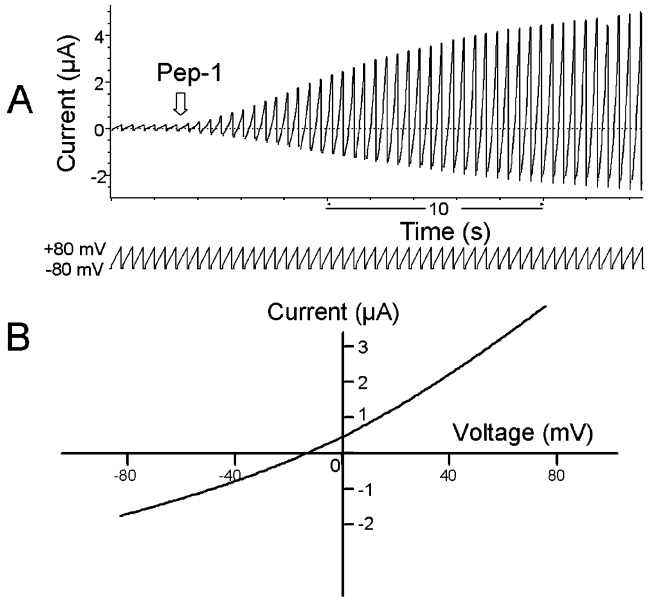

FIGURE 10: (A) Oocyte membrane currents were recorded during 450 ms long voltage ramps applied from a holding potential of −80 to +80 mV, every 5 s. Voltage ramps (shown on bottom) and traces are displayed after concatenation for graphic purposes. Addition of Pep-1 (10 μM) directly to the recording chamber (arrow) induced a marked increase in membrane conductance that developed after 5−10 s. (B) Macroscopic current−voltage curve measured during application of Pep-1 using a voltage-ramp from −80 to +80 mV. The current is shown after digital subtraction of leak current recorded before peptide application. The reversal potential is −8 mV.

(the usual holding potential) to +80 mV (see Figure 10 A). The reversal potential for the Pep-1 induced current was close to −8 mV (Figure 10B), similar to what has already been found for other pore-forming peptides selective for monovalent cations (*31*). Taken together, these results suggested that the permeabilizing capabilities of Pep1 are due to the formation of membrane ion channels.

DISCUSSION

The cell-penetrating peptide Pep-1 was recently described as a powerful agent for the delivery of peptides and proteins through noncovalent interactions, both in vitro and in vivo (*14*). In the present study, we have combined different spectroscopic approaches together with membrane technology to investigate the conformation of Pep-1 and dissect its mechanism of interaction with the cell membrane. We have shown that Pep-1 strongly interacts with lipids and that this interaction is associated with a conformational transition to a helical form. In contrast, formation of Pep1/cargo complexes does not involve any conformational changes of the carrier.

Studies aimed at identifying conformational transitions of CPPs, which occur upon interaction with the membrane, are crucial to understand their mechanism of action and to improve their efficiency. Despite the myriad of studies on CPPs, very little is actually known concerning their membrane translocation mechanism. Moreover recent studies have reevaluated the mechanism of several CPPs, suggesting that the definition of a CPP should be used more carefully (*41*). CPPs described so far seem to adopt different conformational states associated with and required for cellular uptake.

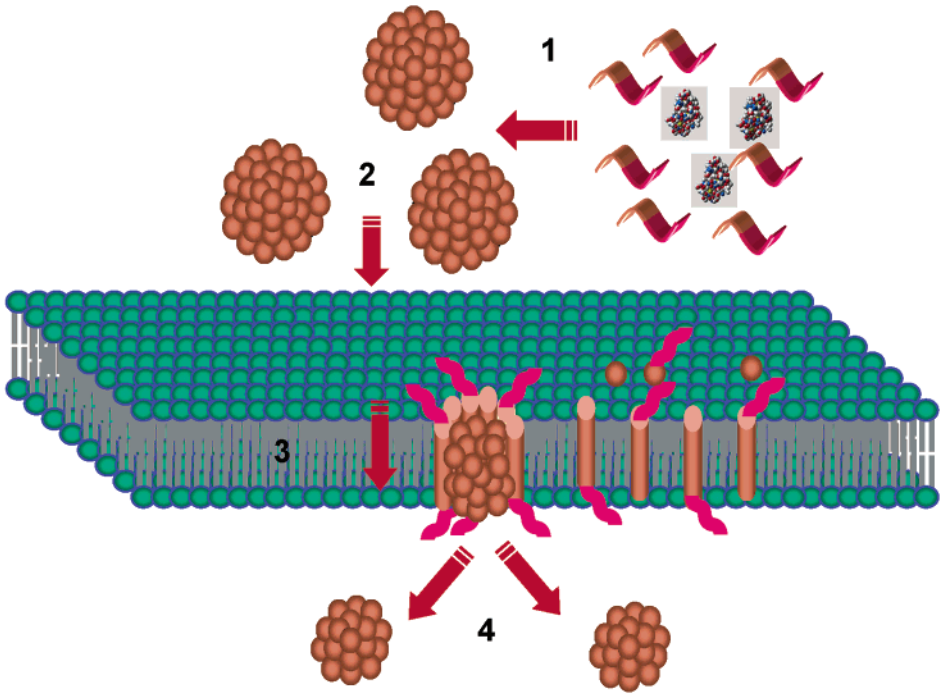

FIGURE 11: Proposed schematic model for translocation of the Pep-1/cargo complex through phospholipid bilayers. The four steps correspond to (**1**) formation of the complex, (**2**) membrane uptake of the complex, (**3**) translocation through the bilayer, and (**4**) release into the cytoplasmic side.

Transportan adopts a helical structure irrespective of the presence or of the nature of the lipids (*22*). In contrast, Tat-derived peptide does not adopt any secondary structure (*8*). pAntp exhibits a structural conversion from helical to β strand in certain circumstances (*42*).

Two important criteria have to be considered in the characterization of CPPs: (i) interactions with lipids and (ii) structural requirements for cellular uptake. Pep-1 adopts a helical fold in the presence of lipids, irrespective of their nature. Both CD observations on transferred monolayers and FTIR investigations carried out on multilayer systems reveal that in the presence of phospholipids, no or nearly no β sheet structure is formed and that the major ordered conformational state corresponds to a helical form. The lipid-induced formation of the helical structure can be associated with hydrophobic interactions. On the contrary, when in water at high dilution, no or very few intermolecular interactions occur and thus, no peptide folding was detected. However, intermolecular interactions similar to those occurring with lipids arise with increasing concentrations of Pep-1, and similarly favor conversion to a helical form. Hydrophobic interactions between Pep-1 and lipids were confirmed by fluorescence experiments. We found that binding of Pep-1 to lipid was associated with an important blue shift of 22 nm, consistent with the insertion of Pep-1 into a hydrophobic environment. Taken together, these data reveal that the structural behavior of Pep-1 is different from that of other CCPs in a lipidic environment. In contrast to pAntp (*42*) and other CPPs containing a hydrophobic domain associated with a NLS (*37*, *38*), no β structure was observed, and no helix to sheet transition was detected. Tat peptide was shown to be unfolded in the presence of lipids (*23*). In the presence of a lipidic enviroment, the behavior of Pep-1 is similar to that of Transportan, the interactions of which with membranes appear to be independent of the nature of the lipids (*21*, *22*).

The helical structure of Pep-1 favors its insertion into the membrane and is therefore most likely directly responsible for the efficiency of its cellular uptake. This hypothesis is conforted by our observation that Pep-1 interacts strongly with lipids. Moreover, the high value found for the cpi suggests that Pep-1 can spontaneously insert into natural membranes and can induce pore formation. Extrapolations shown in Figure 6 also provide a good indication that strong peptide-lipid interactions occur at least in monolayers. In addition, Pep-1 interacts strongly with membranes whatever the nature of the lipid. The fact that a strong association was also observed with neutral lipids suggests than in contrast to Tat-derived peptide or to pAntp, the association with the cell membrane does not involve mainly interactions with headgroup charges. In the case of Tat-derived peptide, glycosaminoglycans on the outer cell surface play a essential role in its interaction with the cell surface. Tat, as well as polyarginine peptides, strongly interact with DOPG, but not with DOPC (*23*). Dom et al. (*43*) have demonstrated that the cellular uptake of pAntp is at least a two-step process, involving initial binding to surface lipids mediated by negatively charged lipids, followed by translocation.

The NMR data have revealed that residues 1−13 of Pep-1 are involved in a helical structure. On the basis of these data, analysis of the helical projection of Pep-1 reveals an amphipathic helix with all of the Trp residues on one side of the helix, whether α or 3_{10}. Such a conformation is also consistent with the crystal structure of a very similar tryptophan rich sequence involved in the dimer interface of HIV 1 reverse transcriptase (*44*). As our fluorescence data indicate that these tryptophan residues are embedded in a hydrophobic environment, it seems likely that Pep-1/ membrane interactions occur with a helical axis perpendicular to the membrane plane.

In conclusion, our conformational and binding analysis associated with the pore-like induced properties of the carrier

peptide Pep-1 has lead us to propose the following model to describe the mechanism of translocation of Pep-1/cargo complexes through the membrane. Pep-1/cargo complexes form independently of any conformational changes within Pep-1. In contrast, interactions with membrane components such as phospholipids generate a helical folding of the carrier which facilitates insertion into the membrane and initiates the membrane translocation process. Since a partial helical folding of Pep-1 also occurs for the Pep-1/cargo complex upon interaction with lipids, although to a lower extent than in its free form, we propose that only the outer part of the Pep-1 "shell" surrounding the cargo is actually involved in interactions with the membrane, and therefore conformationally affected. Formation of the helical form perpendicular to the membrane suggests the formation of a transient transmembrane pore-like structure as schematically shown in Figure 11. In this scheme the four steps correspond to the following: **1**, association between the cargo (peptide or protein) and the vector peptide leading to the formation of a complex; **2**, membrane uptake of the complex at the external side of the cell; **3**, insertion of the complex into the membrane associated with partial conformational changes and pore formation; **4**, release of the complex into the cytoplasm with partial decaging of the cargo.

REFERENCES

1. Ford, K. G., Souberbielle, B. E., Darling, D., and Farzaneh, F. (2001) Protein transduction: an alternative to genetic intervention? *Gene Ther. 8*, 1−4.
2. Wadia, J. S., and Dowdy, S. F. (2002) Protein transduction technology, *Curr. Opin. Biotechnol. 13*, 52−56.
3. Morris, M. C., Chaloin, L., Heitz, F., and Divita, G. (2000) Translocating peptides and proteins and their use for gene delivery, *Curr. Opin. Biotechnol. 11*, 461−466.
4. Gariepy, J., and Kawamura, K. (2001) Vectorial delivery of macromolecules into cells using peptide-based vehicles, *Trends Biotechnol. 19*, 21−28.
5. Lindgren, M., Hällbrink, M., and Langel, Ü. (2002) Quantification of cell-penetrating peptides and their cargoes, in *Cell-Penetrating Peptides: Processes and Applications* (Langel, Ü., Ed.) pp 263−275, CRC Press, Boca Raton, FL.
6. Schwarze, S. R., and Dowdy, S. F. (2000) In vivo protein transduction: intracellular delivery of biologically active proteins, compounds and DNA, *Trends Pharmacol. Sci. 21*, 45−48.
7. (2002) in *Cell-Penetrating Peptides: Processes and Applications*. (Langel, Ü., Ed.) CRC Press, Boca Raton, FL.
8. Schwarze, S. R., Ho, A., Vocero-Akbani, A., and Dowdy, S. F. (1999) In vivo protein transduction: delivery of a biologically active protein into the mouse, *Science 285*, 1569−1572.
9. Gratton, J. P., Yu, J., Griffith, J. W., Babbitt, R. W., Scotland, R. S., Hickey, R., Giordano, F. J., and Sessa, W. C. (2003) Cell-permeable peptides improve cellular uptake and therapeutic gene delivery of replication-deficient viruses in cells and in vivo, *Nat. Med. 9*, 357−362.
10. Derossi, D., Joliot, A. H., Chassaing, G., and Prochiantz, A. (1994) The third helix of the Antennapedia homeodomain translocates through biological membranes, *J. Biol. Chem. 269*, 10444−10450.
11. Elliott, G., and O'Hare, P. (1997) Intercellular trafficking and protein delivery by a herpes virus structural protein, *Cell 88*, 223−233.
12. Pooga, M., Kut, C., Kihlmark, M., Hallbrink, M., Fernaeus, S., Raid, R., Land, T., Hallberg, E., Bartfai, T., and Langel, Ü. (2001) Cellular translocation of proteins by transportan, *FASEB J. 15*, 1451−1453.
13. Futaki, S., Suzuki, T., Ohashi, W., Yagami, T., Tanaka, S., Ueda, K., and Sugiura, Y. (2001) Arginine-rich peptides. An abundant source of membrane-permeable peptides having potential as carriers for intracellular protein delivery, *J. Biol. Chem. 276*, 5836−5840.
14. Morris, M. C., Depollier, J., Mery, J., Heitz, F., and Divita, G. (2001) A peptide carrier for the delivery of biologically active proteins into mammalian cells, *Nat. Biotechnol. 19*, 1173−1176.
15. Gallo, R. C., Burny, A., and Zagury, D. (2002) Targeting Tat and IFN(alpha) as a therapeutic AIDS vaccine, *DNA Cell. Biol. 21*, 611−618.
16. Kowolik, C. M., Yam, P., Yu, Y., and Yee, J.-K. (2003) HIV vector production by Rev protein transduction, *Mol. Ther. 8*, 324−331.
17. Wu, Y., Wood, M. D., Yi, T., and Katagiri, F. (2002) Direct delivery of bacterial a virulence proteins into resistant Arabidopsis protoplasts leads to hypersensitive cell death, *Plant J. 33*, 131−137.
18. Pratt, R. L., and Kinch, M. S. (2002) Activation of the EphA2 tyrosine kinase stimulates the MAP/ERK kinase signaling cascade, *Oncogene 21*, 7690−7699.
19. Aoshiba, K., Yokohori, N., and Nagai, A. (2003) Alveolar wall apoptosis causes lung destruction and emphysematous changes, *Am. J. Respir. Cell. Mol. Biol. 28*, 555−562.
20. Derossi, D., Chassaing, G., and Prochiantz, A. (1998) Trojan peptides: the penetratin system for intracellular delivery, *Trends Cell. Biol. 8*, 84−87.
21. Magzoub, M., Kilk, K., Eriksson, L. E., Langel, Ü., and Gräslund; A. (2001) Interaction and structure induction of cell-penetrating peptides in the presence of phospholipid vesicles, *Biochim. Biophys. Acta 1512*, 77−89.
22. Magzoub, M., Eriksson, L. E., and Gräslund, A. (2003) Comparison of the interaction, positioning, structure induction and membrane perturbation of cell-penetrating peptides and nontranslocating variants with phospholipid vesicles, *Biophys. Chem. 103*, 271−288.
23. Ziegler, A., Blatter, X. L., Seelig, A., and Seelig, J. (2003) Protein transduction domains of HIV-1 and SIV TAT interact with charged lipid vesicles. Binding mechanism and thermodynamic analysis, *Biochemistry 42*, 9185−9194.
24. Ho, A., Schwarze, S. R., Mermelstein, S. J., Waksman, G., and Dowdy, S. F. (2001) Synthetic protein transduction domains: enhanced transduction potential in vitro and in vivo, *Cancer Res. 61*, 474−477.
25. Morris, M. C., Vidal, P., Chaloin, L., Heitz, F., and (1997) Divita, G. A new peptide vector for efficient delivery of oligonucleotides into mammalian cells, *Nucleic Acids Res. 25*, 2730−2736.
26. Wüthrich, K. (1986) *NMR of Proteins and Nucleic Acids*, John Wiley & Sons Inc., New York.
27. Piotto, M., Saudek, V., and Sklenar, V. (1992) Gradient-tailored excitation for single-quantum NMR spectroscopy of aqueous solutions, *J. Biomol. NMR. 2*, 661−665.
28. Van Mau, N., Vie, V., Chaloin, L., Lesniewska, E., Heitz, F., and Le Grimellec, C. (1999) Lipid-induced organization of a primary amphipathic peptide: a coupled AFM-monolayer study, *J. Membr. Biol. 167*, 241−249.
29. Vie, V., Van Mau, N., Chaloin, L., Lesniewska, E., Le Grimellec, C., and Heitz, F. (2000) Detection of peptide−lipid interactions in mixed monolayers, using isotherms, atomic force microscopy, and Fourier transform infrared analyses, *Biophys. J. 78*, 846−856.
30. Morris, M. C., Chaloin, L., Méry, J., Heitz, F., and Divita, G. (1999) A novel potent strategy for gene delivery using a single peptide vector as a carrier, *Nucleic Acids Res. 27*, 3510−3517.
31. Chaloin, L., De, E., Charnet, P., Molle, G., and Heitz, F. (1998) Ionic Channels Formed by Primary Amphipathic Peptides, *Biochim. Biophys. Acta 1375*, 52−60.
32. (1996) in *Circular Dichroism and the Conformational Analysis of Biomolecules*, (Fasman, G. D., Ed.) Plenum Press, New York.
33. Briggs, M. S., Cornell, D. G., Dluhy, R. A., and Gierasch, L. M. (1986) Conformations of signal peptides induced by lipids suggest initial steps in protein export, *Science 233*, 206−208.
34. Tamm, L. K., and Tatulian, S. A. (1997) Infrared spectroscopy of proteins and peptides in lipid bilayers, *Q. Rev. Biophys. 33*, 365−429.
35. Fringeli, U. P., and Fringeli, M. (1979) Pore formation in lipid membranes by alamethicin, *Proc. Natl. Acad. Sci. U.S.A. 76*, 3852−3856.
36. Kennedy, D. F., Crisma, M., Toniolo, C., and Chapman, D. (1991) Studies of peptides forming 3(10)- and alpha-helices and beta-bend ribbon structures in organic solution and in model biomembranes by Fourier transform infrared spectroscopy, *Biochemistry 30*, 6541−6548.

37. Vidal, P., Chaloin, L., Heitz, A., Van Mau, N., Mery, J., Divita, G., and Heitz, F. (1998) Conformational analysis of primary amphipathic carrier peptides and origin of the various cellular localizations, *J. Membrane Biol. 162*, 259−264.
38. Chaloin, L., Vidal, P., Heitz, A., Van Mau, N., Mery, J., Divita, G., and Heitz, F. (1997) Conformations of primary amphipathic carrier peptides in membrane mimicking environments, *Biochemistry 36*, 11179−11187.
39. Demel, R. A., Geurts van Kessel, W. S., Zwaal, R. F., Roelofsen, B., and van Deenen, L. L. (1975) Relation between various phospholipase actions on human red cell membranes and the interfacial phospholipid pressure in monolayers, *Biochim. Biophys. Acta 406*, 97−107.
40. (1983) in *Principles of Fluorescence Spectroscopy*. (Lakowicz, J. R., Ed.) Plenum Press, New York.
41. Richard, J. P., Melikov, K., Vives, E., Ramos, C., Verbeure, B., Gait, M. J., Chernomordik, L. V., and Lebleu, B. (2003) Cell-penetrating peptides. A reevaluation of the mechanism of cellular uptake, *J. Biol Chem. 278*, 585−590.
42. Bellet-Amalric, E., Blaudez, D., Desbat, B., Graner, F., Gauthier, F., and Renault, A. (2000) Interaction of the third helix of Antennapedia homeodomain and a phospholipid monolayer, studied by ellipsometry and PM-IRRAS at the air−water interface, *Biochim. Biophys. Acta 1467*, 131−143.
43. Dom, G., Shaw-Jackson, C., Matis, C., Bouffioux, O., Picard, J. J., Prochiantz, A., Mingeot-Leclercq, M. P., Brasseur, R., and Rezsohazy, R. (2003) Cellular uptake of Antennapedia Penetratin peptides is a two-step process in which phase transfer precedes a tryptophan-dependent translocation, *Nucleic Acids Res. 31*, 556−561.
44. Wang, J., Smerdon, S. J., Jager, J., Kohlstaedt, L. A., Rice, P. A., Friedman, J. M., and Steitz, T. A. (1994) Structural basis of asymmetry in the human immunodeficiency virus type1 reverse transcriptase heterodimer, *Proc. Natl. Acad. Sci. U.S.A. 91*, 7242−7246.

BI035682S